

# Chemically Induced Potential Barriers at the Carbon Nanotube–Metal Nanoparticle Interface

Douglas R. Kauffman and Alexander Star\*

*Department of Chemistry, University of Pittsburgh, Pittsburgh, Pennsylvania 15260*

*Received February 9, 2007; Revised Manuscript Received May 4, 2007*

## ABSTRACT

Single-walled carbon nanotube (SWNT) field effect transistors were electrochemically decorated with Pt, Pd, Au, and Ag nanoparticles. Upon exposure to 10 ppm NO gas in N<sub>2</sub> a trend was found wherein the magnitude of electron transfer into the SWNT valence band scaled with the work function of the individual metal. This trend gives experimental support for the formation of a metal work function dependent potential barrier at the SWNT–nanoparticle interface.

A large amount of interest has been developed concerning the fabrication and application of carbon nanotubes (CNTs) decorated with metal nanoparticles.<sup>1–3</sup> While the use of such nanohybrids is becoming more popular, the intimate electronic relationship between the CNT and deposited metal nanoparticle is still poorly understood. On the other hand, the electronic interactions between CNTs and bulk metal contacts are well described in the literature.<sup>4–6</sup> For example, Dai and co-workers have reported that nanotube field effect transistors (NTFETs) experience sensitivity toward H<sub>2</sub> as a result of modification of the Schottky barrier at the CNT–metal junction.<sup>7</sup> Similarly, H<sub>2</sub> sensitivity was seen in Pd-decorated NTFETs and has been explained in terms of electron donation through H<sub>2</sub> lowering the Pd work function.<sup>8</sup> This explanation relies upon the ability of Pd to dissolve hydrogen and was first suggested in the report of a hydrogen-sensitive metal-oxide-semiconductor FET (MOSFET).<sup>9</sup> However, this explanation may not be complete because it does not give any special consideration to the electronic interaction at the single-walled carbon nanotube (SWNT)–nanoparticle interface. Recently we reported a gas sensor array based on metal-decorated NTFETs that showed unique electronic response for various metal–analyte combinations,<sup>10</sup> but the fundamental mechanism behind the signal transduction remained unclear.

By exposing NTFET devices decorated with different metals to a single gas, one could monitor the electronic response as a function of metal work function. Because NO has an unpaired electron in the  $2\pi^*$  orbital, it is an ideal candidate for probing metal surfaces, and the literature abounds with reports of NO–metal interactions.<sup>11</sup> In this report we compare the behavior of NTFETs decorated with

Pt, Pd, Au, and Ag nanoparticles upon exposure to NO gas. We have found that devices decorated with different metals demonstrate unique electronic behavior upon exposure to NO gas in N<sub>2</sub>. On the basis of our experimental findings we show a correlation between the metal work function of the nanoparticle and magnitude of electronic transfer into the SWNT network of the NTFET device which points toward a work function dependent potential barrier at the SWNT–nanoparticle interface.

Previous reports describe the fabrication of NTFET devices,<sup>12</sup> but briefly, SWNTs were grown via chemical vapor deposition (CVD) onto Si wafers and interdigitated Au/Ti electrodes were photolithographically patterned onto the SWNT network. The chips were wire-bonded and packaged in a 40-pin ceramic dual-inline package (CERDIP). The fabrication process creates multiple devices per chip allowing the response of individual devices to be simultaneously monitored.<sup>10</sup> Measurements made with NTFETs composed of random networks of SWNTs are advantageous because random network NTFETs are less prone to failure due to the large number of conduction pathways. Additionally, while random network NTFETs may not provide information on individual nanotube response, as with singly isolated SWNT FETs,<sup>7,8,13,14</sup> they possess an intrinsic averaging effect in that they remove nanotube to nanotube variation due to the combined response of the entire network.<sup>15</sup> NTFET devices were decorated with metal nanoparticles via electrochemical deposition using a CH Instruments electrochemical analyzer by connecting the source and drain pins of a single device and using it as the working electrode in an electrochemical cell.<sup>16</sup> An epoxy coating (Epoxy Technologies) was used to isolate device leads from the rest of the electrochemical cell to ensure metal deposition only on

\* Corresponding author. E-mail: astar@pitt.edu.

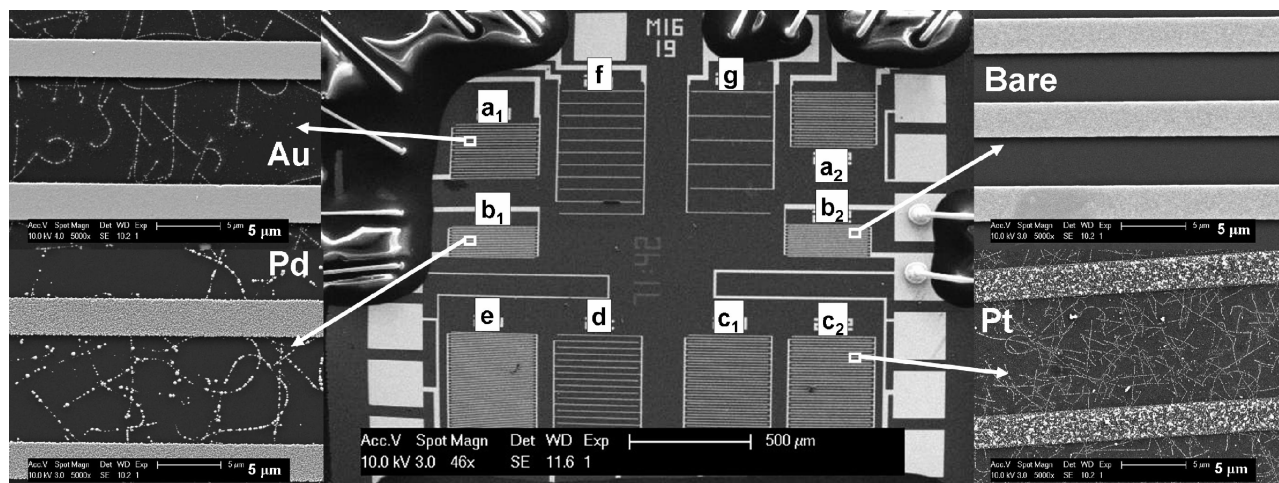


**Figure 1.** SEM images showing multiple interdigitated device geometries present on the NTFET chips (center) and selective Au deposition on device  $a_1$ , Pd deposition on device  $b_1$ , and Pt deposition on device  $c_2$  while the complementary degenerate devices remained bare, as shown with device  $b_2$ .

individual device surfaces. A single drop ( $\sim 100 \mu\text{L}$ ) of 1 mM  $\text{H}_2\text{PtCl}_6$ ,  $\text{HAuCl}_4$ ,  $\text{AgNO}_3$ , or 0.5 mM  $\text{K}_2\text{PdCl}_6$  (Sigma Aldrich) in a supporting electrolyte of 0.1 M  $\text{HCl}$  or  $\text{KNO}_3$  (for  $\text{AgNO}_3$ ) was placed on the NTFET chip with  $\text{Ag}/\text{AgCl}$  reference and Pt wire counter electrodes just in contact with the surface of the solution to create a miniaturized electrochemical cell. A deposition potential of  $-1.0 \text{ V}$  was held for a time between 10 and 90 s to deposit metal nanoparticles of various sizes on the device SWNT networks. Scanning electron microscopy (SEM) was performed with a Phillips XL30 FEG microscope equipped with an EDAX assembly for energy dispersive spectroscopy (EDS) allowing confirmation of metal deposition. For experiments, chips were tested using a custom NTFET electronic test fixture<sup>10</sup> where research grade  $\text{N}_2$  and 10.0 ppm NO gas in  $\text{N}_2$  (Valley National Gas) were passed over the metal-decorated chips and conductance versus gate voltage ( $G-V_G$ ) transfer characteristics of all devices were simultaneously recorded at room temperature.

The NTFET chips used in this study contained multiple devices on the surface, as shown in the center of Figure 1, where the epoxy coating (black) is seen surrounding the wire-bonded contacts. Three sets of degenerate devices, each with identical geometry and electrode separation (pitch), were present on each chip; degenerate devices are denoted with subscripts. Through the selective electrochemical deposition of metals it was possible to decorate particular devices while leaving their degenerate devices bare. To demonstrate the device selective decoration, a deposition time of 60 s was used to deposit  $\sim 150\text{--}300 \text{ nm}$  Au nanoparticles on device  $a_1$ , 90 s was used to deposit  $\sim 150 \text{ nm}$  Pd nanoparticles on device  $b_1$ , and 30 s was used to deposit  $\sim 120 \text{ nm}$  Pt nanoparticles on device  $c_2$  while their complementary degenerate devices were left bare. Longer deposition times resulted in a nearly complete loss of NTFET transfer characteristics due to large nanoparticles screening the gate voltage;<sup>10</sup> to reduce this effect, smaller deposition times between 10 and 20 s were used to decorate chips for gas exposure experiments.

Parts A and B of Figure 2 show the  $G-V_G$  transfer characteristics of degenerate devices  $a_1$  and  $a_2$  from chip 1. During deposition both devices were in the  $\text{HAuCl}_4/\text{HCl}$  solution; Figure 2A shows that after device  $a_1$  was held at potential for 20 s it experienced modest  $G-V_G$  modification whereas Figure 2B shows the  $G-V_G$  transfer characteristic of device  $a_2$  (not held at potential) remained essentially unchanged. This indicates Au nanoparticles were selectively deposited on device  $a_1$ , while  $a_2$  remained pristine. Figure 2C shows the modification of chip 1 devices  $c_1$  and  $c_2$  transfer characteristics resulting from different Pt deposition times. Both devices were independently held in the  $\text{H}_2\text{PtCl}_6/\text{HCl}$  solution at  $-1.0 \text{ V}$  for different amounts of time; device  $c_2$  was held at potential for 20 s, while device  $c_1$  was only held at potential for 10 s to obtain a smaller Pt coverage on the SWNT surface. It can be seen that while device  $c_1$  experienced modest  $G-V_G$  modification, device  $c_2$  experienced an almost complete loss of gate voltage dependency due to increased Pt deposition time. Subsequent SEM images show small Pt nanoparticles around 20 nm in diameter in device  $c_1$  (Figure 2D) and comparatively large 50–100 nm diameter particles in device  $c_2$  (Figure 2E). These results are representative of the  $G-V_G$  modifications seen in devices on both chips upon electrodecoration and are in line with previous reports of metal deposition on NTFET devices.<sup>10</sup> Additional  $G-V_G$  transfer characteristics showing device decoration can be found in the Supporting Information section, Figures S2 and S3.

$G-V_G$  transfer characteristics of all devices on a particular NTFET chip were simultaneously monitored under a 300 SCCM flow of dry  $\text{N}_2$  and 10 ppm NO in  $\text{N}_2$ . The flow system was flushed with dry  $\text{N}_2$  for 1 h prior to NO exposure to remove any  $\text{O}_2$  or humidity present from atmospheric exposure during insertion of the NTFET chip. Removal of  $\text{O}_2$  and trace  $\text{H}_2\text{O}$  from the flow system was necessary to ensure NO did not undergo any Red/Ox reactions in transit to the chip. Initially NO exposure caused a positive shift in device gate voltage which reversed and stabilized upon further exposure. We hypothesize that NO consumed surface-

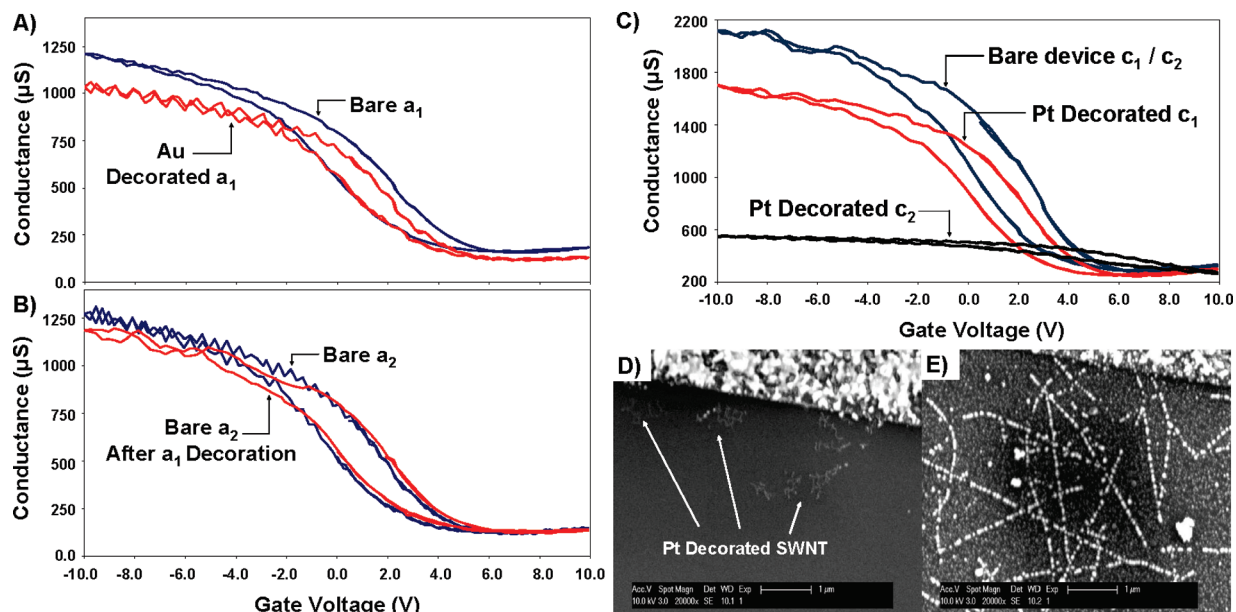


**Figure 2.**  $G-V_G$  transfer characteristics of (A) device  $a_1$  and (B) device  $a_2$  before and after selective Au deposition on device  $a_1$ . It can be seen that Au deposition caused a slight tilt in  $G-V_G$  curve of device  $a_1$  while the undecorated device  $a_2$   $G-V_G$  curve does not significantly change, indicating selective Au deposition only on device  $a_1$ . (C)  $G-V_G$  modification of Pt-decorated devices  $c_1$  and  $c_2$  due to different deposition times; devices  $c_1$  and  $c_2$  were held at  $-1.0$  V for 10 and 20 s, respectively. SEM images of device  $c_1$  (D) showing small ( $\sim 20$  nm) Pt nanoparticles and (E) showing larger (50–100 nm) Pt nanoparticles, illustrating how larger metal nanoparticles distort the device  $G-V_G$  curve.

bound oxygen species on the metal nanoparticle and, by producing electron-withdrawing  $NO_2$ , caused the positive shift in device gate voltage.<sup>10</sup> Further NO exposure depleted the surface-bound oxygen and eventually resulted in a NO-saturated equilibrium on the nanoparticle surface. A conductance versus time plot showing the temporary evolution of  $NO_2$  from an Ag-decorated device in a NO/ $N_2$  environment can be found in the Supporting Information section, Figure S4.  $NO_2$  production time varied depending on the metal species, but an exposure time of 1 h was used for all experiments to ensure measurement in a homogeneous atmosphere and equilibrium state NO coverage on the nanoparticle. As NO has an unpaired electron it is expected to be a weak electron donor, and after the device transfer characteristics stabilized, it was found exposure to 10 ppm NO resulted in a small decrease in conductance and negative shift in gate voltage for all devices on the same chip, with metal-decorated devices showing consistently larger gate voltage shifts.

Figure 3 shows the representative response of chip 1 devices  $a_2$  (bare) and  $a_1$  (Au decorated) upon exposure to dry 10 ppm NO in  $N_2$ .<sup>17</sup> It can be seen that NO exposure caused a smaller gate voltage shift in the bare device  $a_2$  (Figure 3A) compared to the Au-decorated device  $a_1$  (Figure 3B), indicating increased electronic donation into the SWNT network of device  $a_1$ . Without extensive passivation techniques<sup>18</sup> to isolate the device contacts, it is difficult to determine if the small response of bare devices originates from NO interaction with the SWNT network or contacts; however, the deposited metal nanoparticles and bulk NTFET contacts are both composed of Au which suggests the increased gate voltage shift in the Au nanoparticle decorated device is due to an NO–nanoparticle interaction. The  $G-V_G$

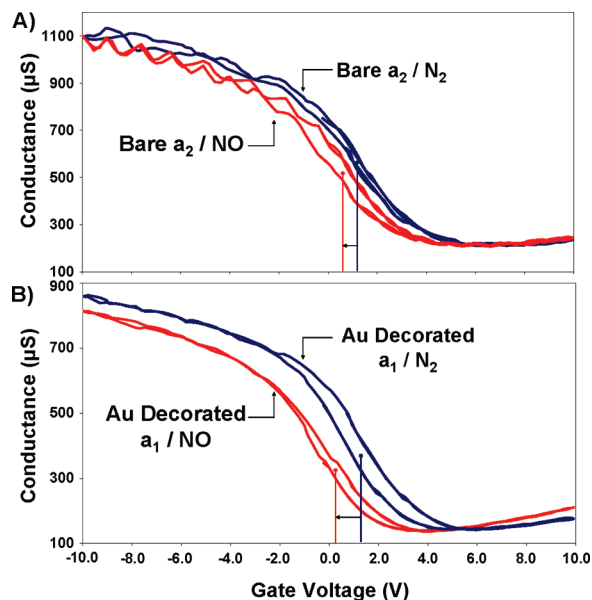


**Figure 3.**  $G-V_G$  response of (A) bare device  $a_2$  and (B) Au-decorated device  $a_1$  to 10 ppm NO gas in  $N_2$ . Increased gate voltage shift indicates increased electron transfer into the SWNT network of the Au-decorated device  $a_1$ .

transfer characteristics of six bare devices and three metal-decorated devices were monitored on two NTFET chips during gas exposure. For a particular chip it was found that bare devices with different geometries and electrode separations (pitch) showed consistent gate voltage shifts, and metal decorated devices all demonstrated unique gate voltage shifts larger than the bare devices (shown in the Supporting Information section, Tables S1 and S2 and Figures S5 and S6). Additionally, the gate voltage shifts in metal-decorated



**Table 1.** Summary of Gate Voltage Shifts of Device Response before and after Metal Decoration

	device	pitch ( $\mu\text{m}$ )	metal	deposition time (s)	particle size (nm)	work function (eV)	gate voltage shift (V)
chip 3	all	5–100	bare	0	N/A	N/A	$-0.30 \pm 0.02$
	a1	10	Ag	10	70–140	4.26	–0.84
	a2	10	Ag	20	80–200	4.26	–0.83
	b1	5	Au	10	41–82	$\sim 5.0$	–0.75
	b2	5	Au	20	113–148	$\sim 5.0$	–0.73
	e	5	Pd	10	45–80	5.12	–0.66
	d	25	Pd	20	100–190	5.12	–0.69
	c1	10	Pt	10	40–80	5.65	–0.57
	c2	10	Pt	20	80–200	5.65	–0.55

devices showed a dependency on the metal work function, where larger shifts were seen in devices decorated with smaller work function metals. It was noticed that although the two NTFET chips (chip 1 and chip 2) demonstrated different magnitude responses to NO gas, the trend between smaller work function and increased device gate voltage shift was consistent (shown in the Supporting Information section, Figure S7). After comparing degenerate bare and decorated devices on separate chips, and finding the trend was independent of the particular device geometry, owing to an average nanoparticle density on the nanotube network, all four metals were used to decorate devices on a single chip (chip 3). Two devices on chip 3 were decorated with each metal for either 10 or 20 s (see Table 1 for decoration specifics). Depositing the metals in this manner allowed a direct comparison between metal decorated NTFET devices on one chip, removing the inconsistency in response magnitude between individual chips. Additionally, this allowed the comparison between the metal nanoparticle size and device response to be made for each metal. It was found that devices decorated with a particular metal nanoparticle showed equivalent gate voltage shifts upon NO exposure despite the difference in particle size which indicates that metal work function, and not particle size, influenced electronic donation into the SWNT network.

Each metal-decorated NTFET device had a unique gate voltage shift upon exposure to NO gas, and when the absolute value of the shift was plotted against the metal work function ( $\Phi$ ), a clear trend was found where a smaller work function led to a larger gate voltage shift. Figure 4 shows the relationship between metal work function and absolute value of the voltage shifts in response to NO for metal-decorated devices on chip 3, where hollow and solid labels represent the response of devices held at a deposition time of 10 (solid labels) or 20 s (hollow labels). Mention should be made concerning the discrepancy found in literature values for  $\Phi_{\text{Au}}$ .<sup>19</sup> Common values for  $\Phi_{\text{Pd}}$ ,  $\Phi_{\text{Pt}}$ , and  $\Phi_{\text{Ag}}$ <sup>19d</sup> were used, and in the absence of a consistent value for  $\Phi_{\text{Au}}$ , an appropriate value was picked ( $\sim 5.0$  eV); in light of this discrepancy we contend any reasonable literature value for  $\Phi_{\text{Au}}$  will still show a similar trend as outlined in Figure 4.

To date few papers have investigated the fundamental electronic interactions between CNTs and metal nanoparticles,<sup>13,20</sup> and while Schottky barriers are known to depend on work function<sup>5,6,21</sup> and gas exposure,<sup>22</sup> the description of

the potential barrier at nanoparticle interfaces is still incomplete. Difficulty in applying traditional Schottky junction behavior has led some to suggest that metal nanoparticles create interfacial “Schottky-type” potential barriers on semiconducting substrates,<sup>13,23</sup> and it has been shown experimentally that Au nanoparticles form size-dependent “nano-Schottky” potential barriers on semiconducting substrates that asymptotically approach the macroscopic Schottky barrier.<sup>24</sup> Regardless of the controversy over the nature of the potential barrier existing at a nanoparticle–semiconductor interface, several important observations can be made regarding the electronic interaction at the SWNT–nanoparticle interface.

First, metal decoration creates a characteristic “tilt” in the device transfer characteristic. This has been previously described as a screening effect on the gate voltage, but deformation of the  $G-V_G$  curve geometry can also be attributed to changes in carrier mobility.<sup>25</sup> It is known that Fermi level alignment occurs whenever a metal and semiconductor are placed in contact, resulting in a charge redistribution and the formation of a depletion layer surrounding the metal.<sup>22</sup> The SWNT-supported metal nanoparticle will experience this effect and create localized depletion regions on the SWNT wall.<sup>26</sup> These charge depletion regions should act as charge scattering sites that would create deviation in the hole trajectory, as shown in Figure 5A. The result would be a reduction in charge mobility through the SWNT network, causing the observed tilt in the decorated device transfer characteristic. Because larger ( $\geq 20$  nm) nanoparticles were used, the thickness of the depletion region

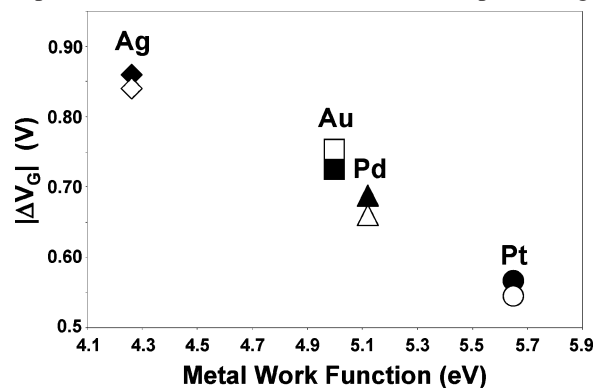


**Figure 4.** Relationship between metal work function and absolute value of observed gate voltage shift in metal-decorated NTFET. Each metal was used to decorate two devices with 10 s (solid labels) and 20 s (hollow labels) deposition time.

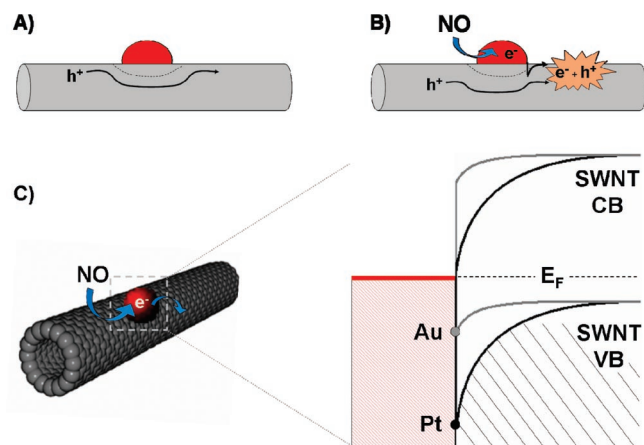


**Figure 5.** (A) Deposition of a metal nanoparticle on the SWNT results in a localized depletion region (dashed line) surrounding the metal nanoparticle; this depletion layer creates an obstacle for hole transport and reduces carrier mobility. (B) Electronic interaction between NO and the metal nanoparticle creates added electronic density on the metal, which after crossing a small potential barrier results in electron–hole recombination—creating a negative shift in the device gate voltage. (C) Expanded view of the electronic interaction occurring at the SWNT–nanoparticle interface. The potential barrier for electron travel into the SWNT valence band is dependent upon the work function of the metal nanoparticle with lower work functions resulting in lower potential barriers for charge recombination.

at the SWNT–nanoparticle interface should not be size dependent,<sup>24,26</sup> therefore decreased charge mobility should be a proportional to SWNT surface coverage. Second, it appears the potential barrier at the SWNT–nanoparticle interface only affects the number of charge carriers upon exposure to NO gas. This can be rationalized by the addition of electronic density into the metal nanoparticle following NO interaction and subsequent electron–hole recombination in the SWNT. As shown in Figure 5B the added electronic density must overcome a small potential barrier to enter the SWNT, whereupon charge recombination occurs—this reduction of hole density in the SWNT is seen as a negative shift in device gate voltage. It was mentioned that the gate voltage shifts of devices decorated with different sized particles were equivalent; this observation is important because it gives experimental evidence that the small potential barrier at the SWNT–nanoparticle interface is not dependent upon nanoparticle size but rather metal work function.

Last, the electronic donation into the SWNT network (negative gate voltage shift) scaled with the work function of the metal, indicating the existence of a metal work function dependent potential barrier between the SWNT and metal nanoparticle. Figure 5C depicts the potential barrier at the SWNT–nanoparticle interface. Due to the much smaller size of the metal nanoparticle, it is rationalized that the metal Fermi level was most affected; therefore the SWNT Fermi level is held constant. With the SWNT Fermi level held constant, the relative scale of the interfacial potential barrier can be correlated to the work function of the metal. Here Au and Pt are used as an example, and it can be seen that a lower work function results in a lower potential barrier; this allows larger electronic density into the SWNT and creates

a larger negative shift in the device gate voltage. Interestingly, similar results were seen in SWNTs end-contacted to bulk metals of similar work function; it was found SWNTs contacted with lower work function metals resulted in negative shifts in the device threshold voltage.<sup>6,27</sup> The main difference between the SWNT-supported metal nanoparticles and bulk metal contacts is that until electronic density is introduced, via molecular interaction, the nanoparticle acts as an inert hole scattering site. Only upon electronic interaction do the SWNT-supported nanoparticles show behavior similar to bulk metal contacts. On the basis of these observations it can be seen that the potential barrier at the SWNT–metal nanoparticle interface is not a traditional Schottky barrier, and the effect of the potential barrier on the device gate voltage is only felt when a molecular bias (electronic interaction) is applied.

Through device selective electrodeposition of Ag, Au, Pd, and Pt nanoparticles, we have shown experimentally that electronic donation into the SWNT network of a NTFET upon exposure to NO gas in N<sub>2</sub> is dependent upon the work function of the metal. Furthermore, we have given evidence that a potential barrier exists at the nanoparticle–SWNT interface that is intimately related to the work function of the metal. While the potential barrier at the SWNT–metal nanoparticle interface does resemble traditional Schottky barriers in some regards, there are several differences that make it stand apart and necessitate unique description. Additionally, it was shown that the SWNT–nanoparticle interfacial potential barrier is not size dependent, as devices decorated with nanoparticles of different sizes gave equivalent gate voltage shifts upon exposure to NO gas. It is now possible to rationalize a metal-decorated SWNT sensor array response as a combination of analyte electronic transfer and the potential barrier at the particular SWNT–nanoparticle, where a work function dependent response should be expected for each metal–analyte interaction. It is hoped further investigation into the intimate electronic relationship between CNTs and metal nanoparticles will lead to the design of more sensitive sensor architectures and higher efficiency catalytic pathways.

**Acknowledgment.** We thank Nanomix Inc. for supplying the NTFET devices used in this study. The authors thank the Department of Materials Science and Engineering for the provision of access to the electron microscopy instrumentation and Dr. P. D. Kichambare and A. Stewart for assistance with the execution of this part of our research.

**Supporting Information Available:** Further data for bare and metal-decorated NTFET devices and electrochemical cell schematic. This material is available free of charge via the Internet at <http://pubs.acs.org>.

## References

- (1) Wildgoose, G. G.; Banks, C. E.; Compton, R. G. *Small* **2006**, *2*, 182.
- (2) Ye, X. R.; Chen, L. H.; Wang, C.; Aubuchon, J. F.; Chen, I. C.; Gapin, A. I.; Talbot, J. B.; Jin, S. *J. Phys. Chem. B* **2006**, *110*, 12938.
- (3) Qu, L.; Dai, L.; Osawa, E. *J. Am. Chem. Soc.* **2006**, *128*, 5523.
- (4) Shan, B.; Cho, K. *Phys. Rev. B* **2004**, *70*, 233405.
- (5) Léonard, F.; Tersoff, J. *Phys. Rev. Lett.* **2000**, *84*, 4693.

- (6) Chen, Z.; Appenzeller, J.; Knoch, J.; Lin, Y.; Avouris, P. *Nano Lett.* **2005**, *5*, 1497.
- (7) Javey, A.; Guo, J.; Wang, Q.; Lundstrom, M.; Dai, H. *Nature* **2003**, *424*, 654.
- (8) Kong, J.; Chapline, M. G.; Dai, H. *Adv. Mater.* **2001**, *13*, 1384.
- (9) Lundström, I.; Shivaraman, S.; Svensson, C.; Lundkvist, L. *Appl. Phys. Lett.* **1975**, *26*, 55.
- (10) Star, A.; Joshi, V.; Skarupo, S.; Thomas, D.; Gabriel, J. -C. P. *J. Phys. Chem. B* **2006**, *110*, 21014.
- (11) Brown, W. A.; King, D. A. *J. Phys. Chem. B* **2000**, *104*, 2578.
- (12) Star, A.; Tu, E.; Niemann, J.; Gabriel, J. -C. P.; Joiner, C. S.; Valcke, C. *Proc. Natl. Acad. Sci. U.S.A.* **2006**, *103*, 921.
- (13) Kim, B. -K.; Park, N.; Na, P. S.; So, H. -M.; Kim, J. -J.; Kim, H.; Kong, K. -J.; Chang, H.; Ryu, B. -H.; Choi, Y.; Lee, J. -O. *Nanotechnology* **2006**, *17*, 496.
- (14) Martel, R.; Schmidt, T.; Shea, H. R.; Hertel, T.; Avouris, P. *Appl. Phys. Lett.* **1998**, *73*, 2447.
- (15) (a) Snow, E. S.; Novak, J. P.; Campbell, P. M.; Park, D. *Appl. Phys. Lett.* **2003**, *82*, 2145. (b) Snow, E. S.; Campbell, P. M.; Ancona, M. G.; Novak, J. P. *Appl. Phys. Lett.* **2005**, *86*, 033105.
- (16) Using the NTFET device as a working electrode allowed cyclic voltammetry measurements; this is further shown in the Supporting Information, Figure S1.
- (17) A general decrease in conductance was noticed when measurements were taken under nitrogen flow as compared to ambient atmosphere; this results from purging the electron-withdrawing O<sub>2</sub> from the flow chamber. For an explanation of CNT sensitivity toward oxygen see: Collins, P. G.; Bradley K.; Ishigami, M.; Zettl, A. *Science*, **2000**, *287*, 1801.
- (18) Zhang, J.; Boyd, A.; Tselev, A.; Paranjape, M.; Barbara, P. *Appl. Phys. Lett.* **2006**, *88*, 123112.
- (19) (a) Anderson, P. A. *Phys. Rev.* **1959**, *115*, 553. (b) Michaelson, H. B. *J. Appl. Phys.* **1950**, *21*, 536. (c) Eastman, D. E. *Phys. Rev. B* **1970**, *2*, 1. (d) Michaelson, H. B. *J. Appl. Phys.* **1977**, *48*, 4729.
- (20) Zhao, Q.; Nardelli, M. B.; Lu, W.; Bernholc, J. *Nano Lett.* **2005**, *5*, 847.
- (21) Heinze, S.; Tersoff, J.; Martel, R.; Derycke, V.; Appenzeller, J.; Avouris, P. *Phys. Rev. Lett.* **2002**, *89*, 106801.
- (22) Zangwill, A. *Physics at Surfaces*; Cambridge University Press: Cambridge, U.K., 1988.
- (23) Kolmakov, A.; Klenov, D. O.; Lilach, Y.; Stemmer, S.; Moskovits, M. *Nano Lett.* **2005**, *5*, 667.
- (24) Ruffino, F.; Grimaldi, M. G.; Giannazzo, F.; Roccaforte, F.; Raineri, V. *Appl. Phys. Lett.* **2006**, *89*, 243113.
- (25) Hecht, D. S.; Ramirez, R. J. A.; Briman, M.; Artukovic, E.; Chichak, K. S.; Stoddart, J. F.; Grüner, G. *Nano Lett.* **2006**, *6*, 2031.
- (26) Ioannides, T.; Verykios, X. E. *J. Catal.* **1996**, *161*, 560.
- (27) Nosh, Y.; Ohno, Y.; Kishimoto, S.; Mizutani, T. *Nanotechnology* **2006**, *17*, 3412.

NL070330I